

Flexural strength of prestressed concrete members with unbonded tendons

Deuck Hang Lee^a and Kang Su Kim*

Department of Architectural Engineering, University of Seoul, Seoul, Korea

(Received July 14, 2010, Accepted April 6, 2011)

Abstract. It is difficult to accurately predict the flexural strength of prestressed members with unbonded tendons, unlike that of prestressed members with bonded tendons, due to the unbonded behavior between concrete and tendon. While there have been many studies on this subject, the flexural strength of prestressed members with unbonded tendons is still not well understood, and different standards in various countries often result in different estimation results for identical members. Therefore, this paper aimed to observe existing approaches and to propose an improved model for the ultimate strength of prestressed members with unbonded tendons. Additionally, a large number of tests results on flexural strength of prestressed members with unbonded tendons were collected from previous studies, which entered into a database to verify the accuracy of the proposed model. The proposed model, compared to existing approaches, well estimated the flexural strength of prestressed members with unbonded tendons, adequately reflecting the effects of influencing factors such as the reinforced steel ratio, the loading patterns, and the concrete strength. The proposed model also provided a reasonably good estimation of the ultimate strength of over-reinforced members and high-strength concrete members.

Keywords: prestressed; post-tension; unbonded; prestressing tendon; flexural strength.

1. Introduction

Prestressed concrete (hereinafter, "PSC") members are widely used in long span structures due to their excellent performance against cracks and deflection. Depending on the time of release, PSC members can be divided into the pre-tensioned members and post-tensioned members, and the post-tensioned members can be further divided into the members with bonded tendons and unbonded tendons. When integrated construction is required as in most statically indeterminate structures, the post-tension method is often used. In such cases, unbonded tendons are widely applied as they require no grouting work after release, and thus offer an easy construction.

When the unbonded tendons are applied, however, as opposed to the bonded tendons, the strain compatibility condition between concrete and tendon cannot be utilized due to the unbonding behavior. Thus, it is difficult to accurately analyze flexural strength because the stress of unbonded tendons is hard to obtain from the sectional strain of concrete at the tendon level (Collins and Mitchell 1991). While there have been many studies on this issue (Janney *et al.* 1956, Warwaruk *et al.*

*Corresponding author, Associate Professor, E-mail: kangkim@uos.ac.kr

^aPh.D. Candidate

1962, Bondy 1970, Tam and Pannell 1976, Du and Tao 1985, Macgregor *et al.* 1989, Harajli 1990, Harajli and Kanj 1991, Campbell and Chouinard 1991, Naaman and Alkhairi 1991, Lee *et al.* 1999, Chakrabarti 1995, Allouche *et al.* 1999, Ng 2003, Au and Du 2004, Robert-Wollmann *et al.* 2005, Harajli 2006, Sivaleepunth *et al.* 2006, Bui and Niwa 2006, Tan and Tjandra 2007, Ozkul *et al.* 2005, Du *et al.* 2008, Ozkul *et al.* 2008, Au *et al.* 2009, Zhou and Zheng 2010), our understanding on the flexural strength of unbonded post-tensioned (hereinafter, "UPT") members are still very limited and, consequently, countries adopt different standards (DIN 4227 1980, NEN 3880 1984, BSI 8110-85 1985, CAN-A23.3-M94 1994, AASHTO 2004, ACI Committee 318 2005, 2008, KCI-M-07 2007) resulting in quite a large difference among them (See also Appendix for various approaches). For example, the equation for predicting the ultimate stress of UPT members presented in ACI 318M-05 and -08 (2005, 2008), which Mojtahedi *et al.* (1978) first proposed in 1978, offers a relatively safe value but a low level of accuracy.

Therefore, this study reviews existing approaches for the prediction of the ultimate strength of UPT members and proposes a more rational and improved model. The proposed model efficiently reflects the effects of variables such as the loading pattern, the concrete strength (f'_c), the amount of tensile steel (A_s), the amount of compression steel (A'_s), the amount of tendons (A_{ps}), the effective prestress (f_{pe}), and the length of the maximum moment zone. Additionally, this paper established a database of 177 test results from previous studies, which is used to verify the accuracy of the proposed model.

2. Research significance

This study conducted a thorough analysis of existing methods that researchers have proposed for the prediction of the ultimate tendon stresses of UPT members, and derived a rational method. The flexural strength model for UPT members proposed in this paper used the simplified maximum curvature distribution and implemented the moment distribution coefficient to reflect the loading pattern. Also, the accuracy of the proposed method was evaluated using a database having 177 test results from previous studies. The result showed that the proposed method well predicted the flexural strength of UPT members adequately reflecting the effect of primary factors such as the reinforcement ratio, the loading type, and the concrete strength.

3. Review of previous researches

There have been various studies on the flexural strength of UPT members in Europe and North America since the early 1960s. Warwaruk *et al.* (1962) performed an experiment on UPT members with primary test variables of the amount of bonded reinforcing bars and loading patterns (or shape of bending moment distribution). Based on the test results, they proposed a semi-empirical equation for ultimate tendon stresses introducing the bonded reinforcing steel coefficient and the moment area coefficient. Particularly, they verified that the existence of bonded reinforcing steel is a key factor in flexural strength of UPT members, and introduced the virtual strain concept to calculate the ultimate strains of unbonded tendons.

Cambell *et al.* (1991) also confirmed that the amount of the bonded reinforcing bars greatly affected the ultimate strains of tendons, and Chakrabarti (1995) as well as Du and Tao (1985) also

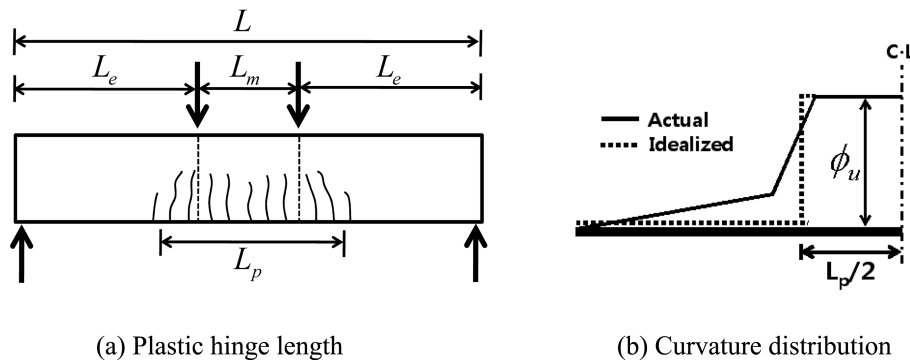


Fig. 1 Plastic hinge model (Harajli 1990, Campbell and Chouinard 1991, Lee *et al.* 1999, Ozkul *et al.* 2008)

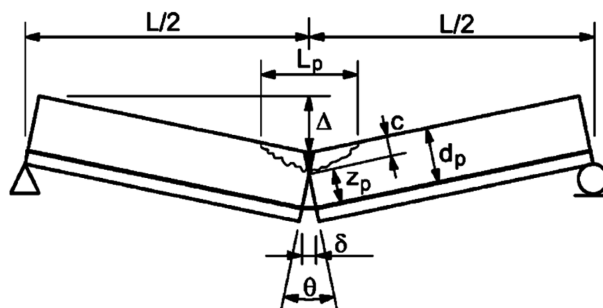


Fig. 2 Rigid-body model (Macgregor *et al.* 1989, Harajli 2006, Robert-Wollmann *et al.* 2005)

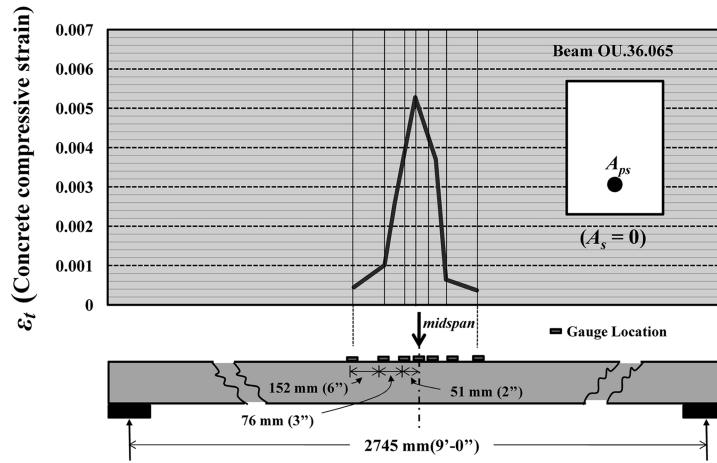
proposed equations that reflect the effect of bonded reinforcing bars. Bondy (1970) observed that the vertical displacement of members directly causes stress changes in tendons. Thus, he proposed an empirical equation for estimation of tendon stresses based on the assumption that tendon stresses increase linearly as elastic deflection of UPT member increases.

Allouche *et al.* (1999) proposed the numerical model using the finite element program, which is capable of predicting response of continuous UPT members from service load to ultimate. Based on the analysis results, a design equation was proposed considering loading patterns, member continuity and confine effect of concrete.

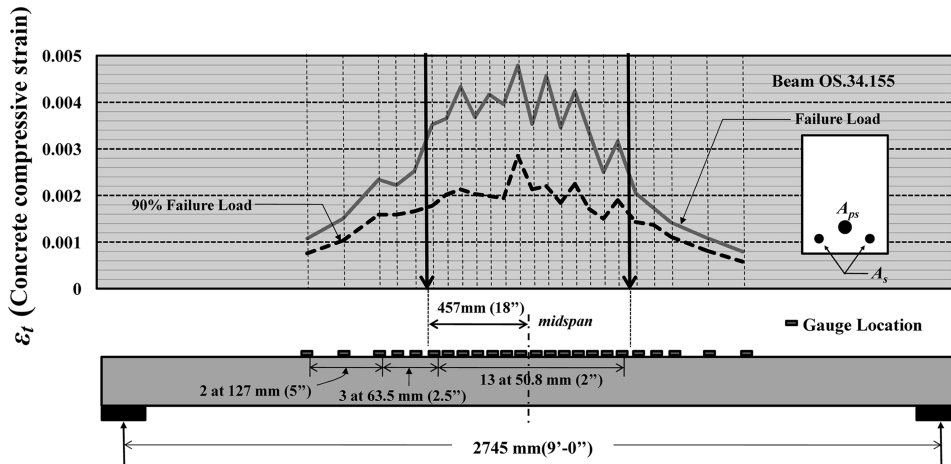
Harajli (1990) proposed the concept of equivalent plastic hinges with idealized curvature distribution, as shown in Fig. 1, which were estimated to be at least larger than the length of the maximum moment zone by over half of the member depth. Au and Du (2004) also applied the concept of equivalent plastic hinges to continuous beams. Based on the equivalent plastic hinge model, Bui and Niwa (2006) and Lee *et al.* (1999) performed a regression analysis of ultimate tendon stresses (f_{ps}) and proposed a strength prediction model and a design equation.

Macgregor *et al.* (1989) presented the rigid body model, wherein all plastic deformations at ultimate state are concentrated on a particular section in the plastic hinge region as shown in Fig. 2. Later, Robert-Wollmann *et al.* (2005) and Harajli (2006) also complemented this rigid body model in their research.

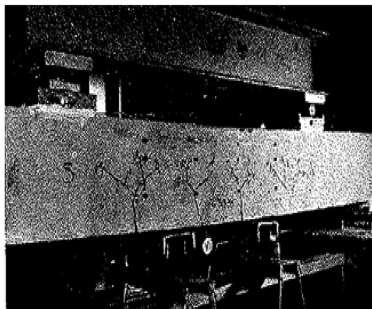
Naaman and Alkhairi (1991a, b) proposed a design equation that considers not only the sectional properties but also the tendon profile, in which loading patterns and the reduction of bond



(a) Measured compressive strains along the length of a prestressed beam WITHOUT bonded reinforcement under a concentrated loading



(b) Measured compressive strains along the length of a prestressed beam WITH bonded reinforcement under 2 points loading



(c) Crack distribution along the length of a prestressed beam WITHOUT bonded reinforcement under 2 points loading

Fig. 3 Experimental test results by Warwaruk *et al.* (1962)

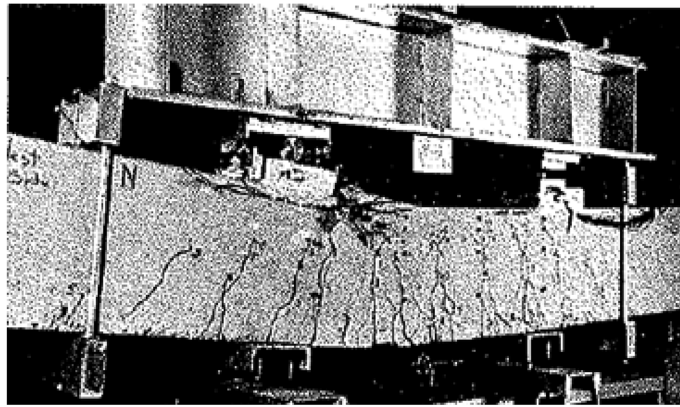


Fig. 4 Failure of a prestressed test beam with unbonded tendons and bonded reinforcement (Warwaruk *et al.* 1962)

characteristics between concrete and tendons are also considered. Later, Ng (2003) proposed modified bond coefficients to reflect the second-order effects based on Naaman and Alkhairi (1991b)'s model for the evaluation of the flexural strength of externally prestressed beams.

The common feature among many of these models for UPT members that have been developed so far is that the plastic hinge length is considered as a key factor in determining the increase of the ultimate tendon stresses. Particularly, the models based on the rigid body model assume that all deformations are concentrated on the particular section in the plastic hinge region, and, therefore, the stress increase of tendons at ultimate is determined by the plastic rotation angle (θ) and the depth of the neutral axis (c).

Fig. 3(a) shows a test result presented by Warwaruk *et al.* (1962), and provides the measured concrete compressive strain at ultimate in a UPT member without bonded reinforcing steel subjected to a concentrated load. It shows that all deformations are concentrated on a section, which supports the afore-mentioned assumption of the rigid body model. Fig. 3(b), however, which is another test result performed by Warwaruk *et al.* (1962), is different from Fig. 3(a)—that is, the measured concrete compressive strains of extreme top fiber shown in Fig. 3(b) are equally distributed within the maximum moment zone, which means that the length of the plastic region significantly differs from that in Fig. 3(a). There are two reasons for this: first, the specimen shown in Fig. 3(b) had reinforcing steel bars while that in Fig. 3(a) did not, and second, it was subjected to two-points loading while that that in Fig. 3(a) was under a concentrated load. In the case of the specimen in Fig. 3(b), it is considered that tensile cracks were distributed in a wide region and well controlled due to the bonded reinforcing steel, which eventually affected the length of the plastic hinge over the length of the maximum moment zone.

Considering, however, the pattern of the cracks at failure in the UPT member without bonded reinforcing bars under two-points loading, as Fig. 3(c) shows, bared another difference. The cracks on the beam without bonded reinforcing steel shown in Fig. 3(c) are not concentrated in one section, though few, but are distributed within the maximum moment region. The cracks were neither well distributed, as they were on the beam with bonded reinforcing steel shown in Fig. 4, nor were they concentrated in a section, as they were on the beam without bonded reinforcing steel shown in Fig. 3(a). The difference between the specimens shown in Fig. 3(c) and Fig. 3(a) is the loading pattern. This means that, although the existence of bonded reinforcing steel affect the extent

Table 1 Estimation of plastic hinge lengths proposed in the previous studies

Researcher	Equation	Eq. No.
Ozkul <i>et al.</i> (2008) and Harajli (1990)	$L_p = L/f + (0.5d_p + 0.05Z)$ where, Z: the shear span length, $f = \infty$ for 1 point loading, $f = 3$ for 2 points loading, $f = 6$ for uniform loading.	(1)
Harajli (2006)	$L_p = (20.7/f + 10.5)c_y$ where, c_y : neutral axis depth at yielding.	(2)
Robert-Wollmann <i>et al.</i> (2005)	$L_p = 10.3c_y$ where, c_y : neutral axis depth at yielding.	(3)
Bui and Niwa (2006)	$L_p = \left[\left(\frac{1 + \omega_s}{\beta_1 L / d_p} \right) + \omega_s + 0.05(-1)^n \right] L$ where n : $n=1$ for 1 point loading, $n=2$ for 2 or uniform loading.	(4)

*Notations that are not specifically mentioned can be found in notation part.

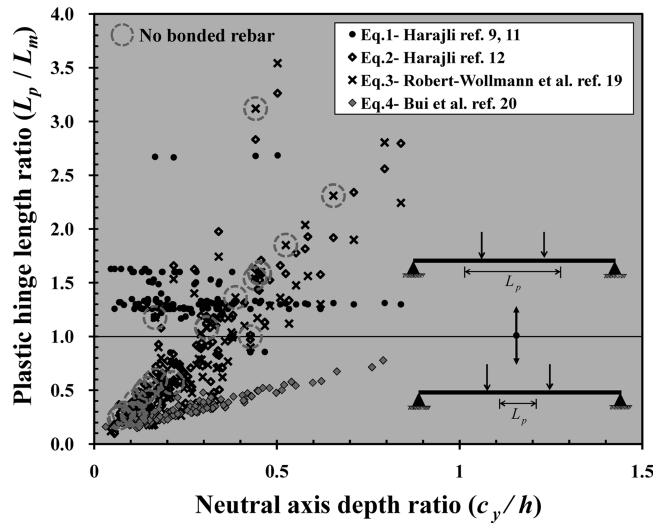


Fig. 5 Comparison of plastic hinge lengths by different approaches (L_p/L_m vs. c_y/h)

of deformation concentration or the length of plastic hinge, the loading pattern, which determines the length of the maximum moment zone, may affect more.

Table 1 shows representative examples of the equivalent plastic hinge lengths proposed in previous researches, and Fig. 5 shows the value L_p/L_m , wherein the length of the plastic hinge (L_p) that was calculated from the these equations is divided by the length of the maximum moment zone (L_m). Eq. (1), shown in Table 1, was proposed by Harajli (1990) and Ozkul *et al.* (2008) wherein the plastic hinge length is always expressed larger than the maximum moment zone by $(0.5d_p + 0.05Z)$. Most of the L_p/L_m values based on Eq. (1), as Fig. 5 shows, are distributed between 1.0 and 1.7. While this means that Eq. (1) reflects the plastic hinge length for the members with

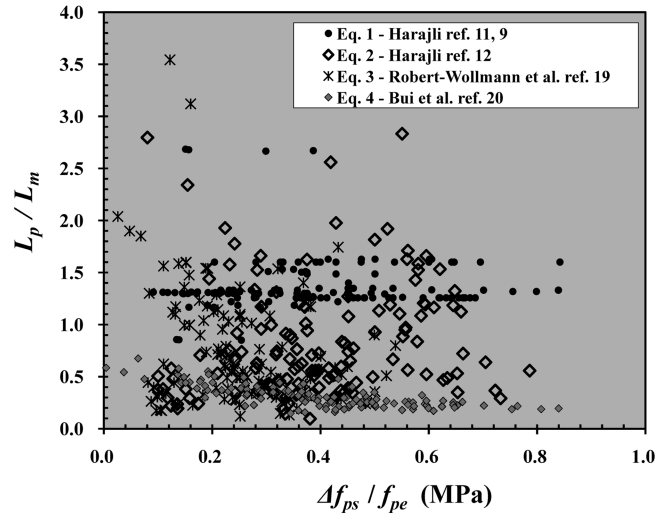


Fig. 6 Relation between L_p/L_m and $\Delta f_{ps}/f_{pe}$

bonded reinforcing steel, it may not properly consider the plastic hinge length for members without bonded reinforcing steel where cracks are either concentrated at a section or distributed within the maximum moment zone. Meanwhile, Eqs. (2) and (3) in Table 1 imply that the plastic hinge lengths tend to increase linearly in proportion to the neutral axis depth ratio (c_y/h) as shown in Fig. 5. While the plastic hinge length is less than the length of maximum moment zone ($L_p/L_m \leq 1$) in some specimens, it is greater than the length of maximum moment zone ($L_p/L_m > 1$) in many others. The specimens expressed with dotted circles are those without the bonded reinforcing steel; and even with these members, Eqs. (2) and (3) estimated the plastic hinge length greater than the length of maximum moment zone ($L_p/L_m > 1$). This reveals that these equations do not well consider the type of failure in members without bonded reinforcing steel where the plastic hinge is more likely developed within the maximum moment zone. Fig. 5 also shows that the values of L_p/L_m from Eq. (4) are mostly distributed between 0.2 and 0.7, which means that the plastic hinge zone is much shorter than the central maximum moment zone. Therefore, Eq. (4) may only adequately estimate the plastic hinge length of the members without bonded reinforcing steel where cracks are either heavily concentrated in a section or ranged within the maximum moment zone; however, it may not reflect the cases that the cracks and deformations are widely distributed and the plastic hinge zone forms throughout the entire maximum moment zone.

Therefore, from the observations based on the aforementioned representative equations, it can be considered that it is very difficult to accurately estimate the plastic hinge length, which is known as a key factor in the flexural strength of UPT members. To more directly check the effect of the plastic hinge length in relation to the magnitude ratio of increase in the ultimate tendon stress to effective prestress ($\Delta f_{ps}/f_{pe}$), $\Delta f_{ps}/f_{pe}$ is plotted versus L_p/L_m in Fig. 6, as calculated by Eqs. (1) to (4). It seems very difficult to ultimately find a clear or direct relationship between the two factors, $\Delta f_{ps}/f_{pe}$ and L_p/L_m . While this may result from the effect of various factors other than the L_p/L_m value, it still supports the argument that it is very difficult to accurately estimate the plastic hinge length.

4. Proposed ultimate strength model

4.1 Ultimate stresses in unbonded tendons

Fig. 7(a) shows a UPT member under two-points loading, and the strain of the concrete at the tendon height occurs in proportion to the moment as shown in Figs. 7(b) and (c). Therefore, at any arbitrary location in the longitudinal direction, the strain increase of the concrete ($\Delta\varepsilon_{pc}$) at the tendon height after the loading can be expressed, as Fig. 7(d) shows, as

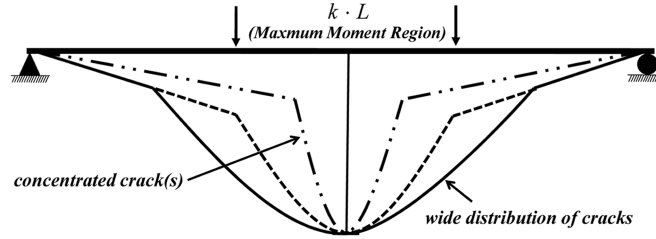
$$\Delta\varepsilon_{pc} = \phi_x(d_p - c_x) \quad (5)$$

where ϕ_x , c_x , and d_p refer to the beam curvature, the depth of the neutral axis, and the distance from extreme compression fiber to centroid of prestressing tendon at an arbitrary location x , respectively. The strain of the tendons, however, as shown in Figs. 7(d) and (e), differs significantly from that in Eq. (5) due to the unbonded behavior between concrete and tendons. In other words, the strain compatibility condition between concrete and tendons implemented for bonded tendons cannot be applied to UPT members. The total magnitude, however, of the change in the length of the tendons between anchorages (ΔL) should be identical to the sum of the concrete strain in longitudinal direction at the height of tendon. Thus, the following relationship is established

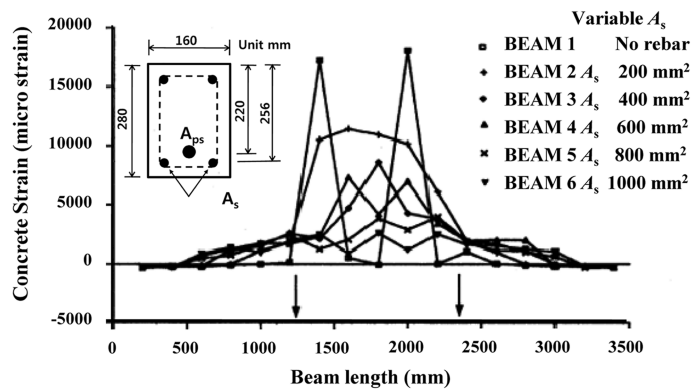
$$\int_0^L \Delta\varepsilon_{pc} dx = \Delta L \quad (6)$$

The curvature distribution of the UPT members at ultimate can be in various shapes, as Fig. 8(a) shows, depending on loading patterns, amount of bonded reinforcing steel, and other characteristics of sectional properties. In general, most of the structural design standards (ACI Committee 318 2005, KCI-M-07 2007) require the minimum amount of bonded reinforcing steel that will prevent brittle failure due to the concentration of cracks for the members with unbonded tendons, which lead cracks to be distributed over the maximum moment region. Therefore, the curvature also tends to be similarly distributed widely over the maximum moment region, and the concrete compressive strain increases significantly in the location with a marked increase in the curvature. The concrete compressive strain on the UPT member in Fig. 8(b), as Campbell and Chouinard (1991) reported, peaked at around the maximum moment zone (that is, the zone between the loading points) at the ultimate load (P_u). In this regard, the curvature distribution of UPT members at ultimate shown in Fig. 8(a) can be represented by the solid line in Fig. 9, noted as original curvature. Additionally, to simplify the calculation, since the curvature outside of the maximum moment zone is considerably smaller than that in the maximum moment zone, the curvature distribution can be idealized as having been concentrated within the maximum moment zone, as the dotted line shows. In other words, this idealization shows that the curvature outside the maximum moment zone is ignored and the curvature within the maximum moment zone is deemed to have a uniform curvature at the maximum moment (ϕ_m). Therefore, using the idealized curvature distribution, the total amount of concrete strain at the tendon level (ΔL) can be expressed as

$$\Delta L = \phi_m(d_p - c_m)kL = \frac{\varepsilon_{cu}}{c_m}(d_p - c_m)kL \quad (7)$$



(a) Distribution of curvature at ultimate



(b) Concrete compressive strains along a UPT member tested by Cambell *et al.* (1991)

Fig. 8 Deformation of UPT members

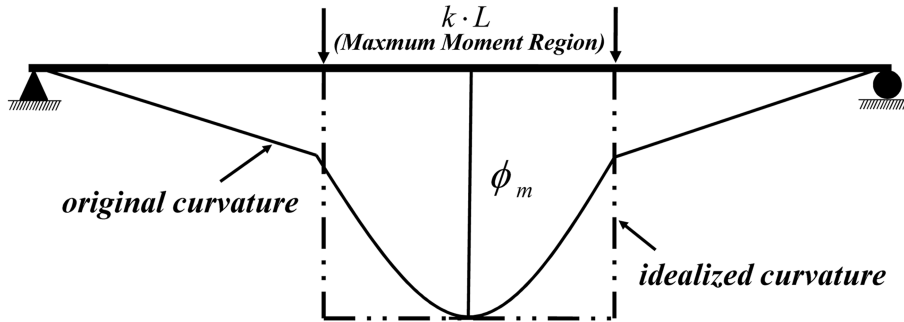


Fig. 9 Idealized curvature for UPT members in this study

where ϕ_m , c_m , and ϵ_{cu} refer to the curvature, the neutral axis depth, the ultimate strain of the concrete in maximum moment region, respectively, and k is the ratio of the maximum moment zone length to the member length.

The average strain increase of the tendon ($\Delta\epsilon_{ps}$) after loading can be calculated by dividing the total amount of the tendon elongation (ΔL) in Eq. (7) by the initial length of the tendon (L), i.e.

$$\Delta\epsilon_{ps} = \frac{\Delta L}{L} = k \frac{\epsilon_{cu}}{c_m} (d_p - c_m) \tag{8}$$

In other words, both the neutral axis and the coefficient of the maximum moment zone (k) determine average strain increase of the tendon ($\Delta\varepsilon_{ps}$) in the proposed method.

The equilibrium of sectional forces at ultimate in the maximum moment zone, as shown in Fig. 7(d), can be derived

$$C = T \quad (9a)$$

$$C = 0.85f'_c b\beta_1 c_m + f'_s A'_s \quad (9b)$$

$$\begin{aligned} T &= f_s A_s + f_{ps} A_{ps} \\ &= f_s A_s + E_p A_{ps} (\varepsilon_{pe} + \Delta\varepsilon_{ps}) \end{aligned} \quad (9c)$$

where c_m and A_{ps} refer to the depth of the neutral axis at ultimate in the maximum moment zone and the area of unbounded prestressing steel, respectively. Other notations that are not mentioned here can be found in the notation part of this paper.

Then, the average strain increase of the tendon ($\Delta\varepsilon_{ps}$) can be expressed from Eqs. (8) and (9) as

$$\Delta\varepsilon_{ps} = \frac{0.85f'_c b\beta_1 c_m + f'_s A'_s - f_s A_s}{E_p A_{ps}} - \varepsilon_{pe} \quad (10)$$

Additionally, substituting Eq. (10) into Eq. (8), the quadratic equation for c_m can be expressed as follows

$$0.85f'_c b\beta_1 c_m^2 - (f_s A_s - f'_s A'_s - k\varepsilon_{cu} E_p A_{ps} + \varepsilon_{pe} E_p A_{ps}) c_m - k\varepsilon_{cu} E_p A_{ps} d_p = 0 \quad (11)$$

Thus, c_m is calculated as follows

$$c_m = \frac{-B \pm \sqrt{B^2 - 4AC}}{2A} \quad (12a)$$

where A , B , and C are

$$A = 0.85f'_c b\beta_1 \quad (12b)$$

$$B = -(f_s A_s - f'_s A'_s - k\varepsilon_{cu} E_p A_{ps} + \varepsilon_{pe} E_p A_{ps}) \quad (12c)$$

$$C = -k\varepsilon_{cu} E_p A_{ps} d_p \quad (12d)$$

Therefore, the strain increase of unbonded tendon at ultimate state ($\Delta\varepsilon_{ps}$) can be calculated by substituting c_m from Eq. (12a) into Eq. (8) or (10).

4.2 Consideration of loading patterns

As aforementioned, the tendon strain is determined by the change in the total member length, which depends on the loading pattern, i.e., the moment shape. The proposed Eqs. (8) to (12) were derived, however, from the assumption of two-points loading condition, and therefore, other loading patterns should be considered. This can be done by considering the moment distribution patterns,

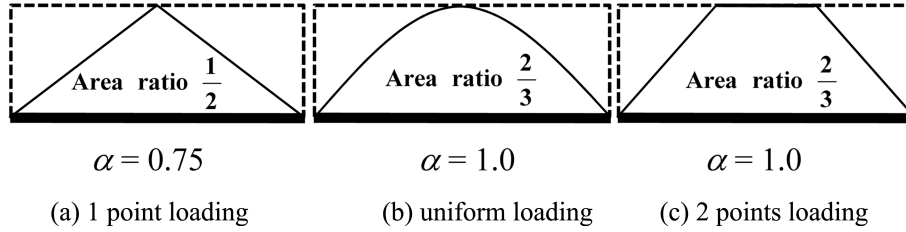


Fig. 10 Coefficients of moment shape (α) for different loading types

for which this study implemented the coefficient of moment shape (α). The coefficient of moment shape (α) can be determined based on its relationship to the area ratio of the bending moment diagram, as Fig. 10 shows, which is 0.75 in the case of the concentrated loading, and 1.0 for the uniformly distributed loading and two-points loading condition. In the case of the two-points loading, however, it should be noted that the coefficient of moment shape (α) was based on the loading points located at the one-third of the member length. In other cases, a more detailed coefficient of moment shape (α) can be estimated and applied using the area ratio of the moment diagram relative to the case of $\alpha = 1.0$.

Thus, introducing the coefficient of moment shape (α) into Eq. (11), it yields

$$0.85f'_c b \beta_1 c_m^2 - (f_s A_s - f'_s A'_s - \alpha k \epsilon_{cu} E_p A_{ps} + \epsilon_{pe} E_p A_{ps}) c_m - \alpha k \epsilon_{cu} E_p A_{ps} d_p = 0 \tag{13}$$

Then, c_m is also obtained by solving the Eq. (13), which is identical to Eq. (12a), except that the value of α is inserted to the Eqs. (12c) and (12d), and the values of B and C are expressed as follows

$$B = -(f_s A_s - f'_s A'_s - \alpha k \epsilon_{cu} E_p A_{ps} + \epsilon_{pe} E_p A_{ps}) \tag{14a}$$

$$C = -\alpha k \epsilon_{cu} E_p A_{ps} d_p \tag{14b}$$

Then, the average strain increase of the tendon ($\Delta \epsilon_{ps}$) can be calculated as follows

$$\Delta \epsilon_{ps} = \alpha k \frac{\epsilon_{cu}}{c_m} (d_p - c_m) \tag{15}$$

Additionally, if the tendon stress is limited to or less than the yield stress (f_{py}) for the conservative estimation of the strength of UPT members, the increase of tendon stress (Δf_{ps}) becomes

$$\Delta f_{ps} \leq f_{py} - f_{pe} = f_{py} - E_p \epsilon_{pe} \tag{16}$$

where ϵ_{pe} and f_{pe} refer to the effective prestrain and prestress in prestressing tendon. The increase of tendon stress at ultimate (Δf_{ps}) can be calculated from the tendon strain ($\Delta \epsilon_{ps}$) in Eq. (15), but should be limited to the Δf_{ps} value specified in Eq. (16). Finally, the ultimate tendon stress (f_{ps}) and strain (ϵ_{ps}) can be calculated as follows

$$f_{ps} = f_{pe} + \Delta f_{ps} \tag{17a}$$

$$\epsilon_{ps} = \epsilon_{pe} + \Delta \epsilon_{ps} \tag{17b}$$

4.3 Flexural strength of prestressed members with unbonded tendons

The sectional forces in compression and tension side can be calculated by applying the equilibrium equation (Eq. (9)), considering the ultimate tendon stress (f_{ps}) from Eq. (17a) and the ultimate concrete strain on the extreme compression fiber of section (ϵ_{cu}) as well as the compressive and tensile stresses of bonded reinforcing steel. Then, the flexural strength of UPT members can be calculated as

$$M_n = C_c \left(c_m - \frac{\beta_1 c_m}{2} \right) + C_s' (c_m - d') + T_s (d - c_m) + T_{ps} (d_p - c_m)$$

$$= 0.85 f_c' b \beta_1 c_m \left(c_m - \frac{\beta_1 c_m}{2} \right) + f_s' A_s' (c_m - d') + f_s A_s (d - c_m) + f_{ps} A_{ps} (d_p - c_m) \quad (18)$$

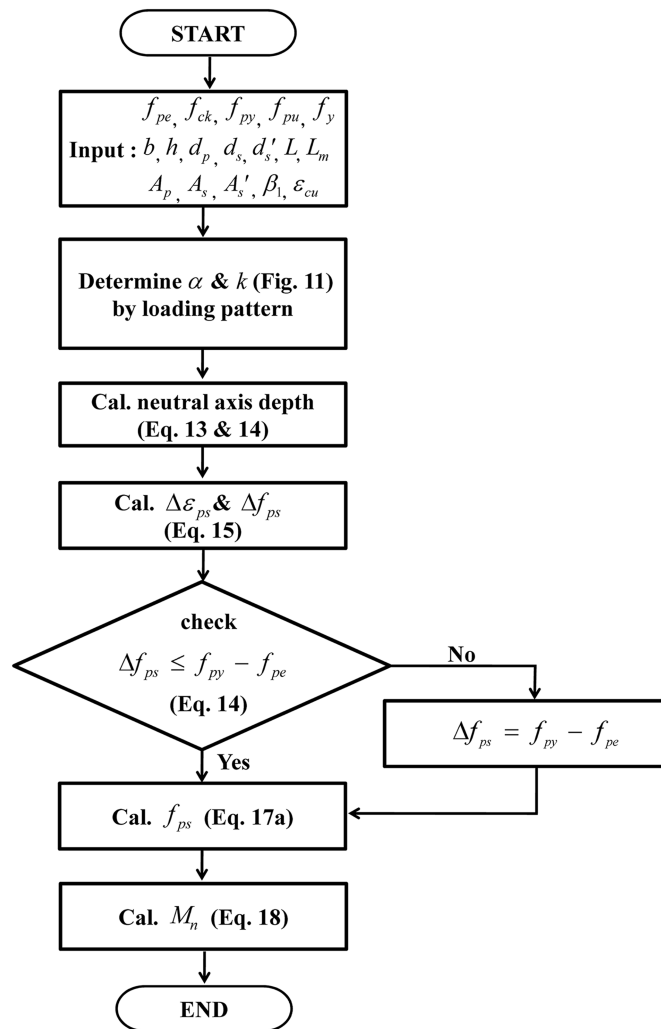


Fig. 11 Flow chart for the calculation of flexural strength of UPT members

where C_c and C_s' , refer to the compression forces of concrete and bonded reinforcing bars, respectively, and T_s and T_{ps} are the tension forces of bonded reinforcing bars and unbonded tendons, respectively. Fig. 11 shows the flow chart to obtain the flexural strength of UPT members including the ultimate tendon stress (f_{ps}) and strain (ε_{ps}) based on the proposed method.

5. Verification of the proposed method

To verify the proposed method on the flexural strength of UPT members, 177 test results were collected from previous researches (Janney *et al.* 1956, Warwaruk *et al.* 1962, Du and Tao 1985, Harajli and Kanj 1991, Campbell and Chouinard 1991, Chakrabarti 1995, Moon *et al.* 2002, Ozkul *et al.* 2005, Ozkul *et al.* 2008) and entered into a database. Table 2 shows the characteristics of the collected data. Over 75% of the data were two-points loaded specimens, and the remaining 25% were one-point or four-points loaded specimens. About 79% of the specimens had bonded reinforcing bars, and the remaining 21% did not have them. The proposed model is considered to perform better for members with bonded reinforcing bars due to the assumption on the curvature at ultimate, but test data on the members without bonded reinforcing bars were also included in the verification to evaluate the applicability of the proposed method with respect to these members as well.

Table 2 Characteristics of test data in the database established in this study

		b (mm)			h (mm)				f_{pe} (MPa)			
range	1 pt.	2 pt.	4 pt.	range	1 pt.	2 pt.	4 pt.	range	1 pt.	2 pt.	4 pt.	
120~160	23	107	0	100~175	0	12	2	750~900	19	54	0	
200~470	10	22	9	225~280	10	76	1	900~1050	4	25	1	
480~600	0	3	3	300~350	23	44	9	1050~1320	10	53	11	
Total	33	132	12	-	33	132	12	-	33	132	12	
		ρ_s (%)			ρ_p (%)				Reinforcement index*			
range	1 pt.	2 pt.	4 pt.	range	1 pt.	2 pt.	4 pt.	range	1 pt.	2 pt.	4 pt.	
0	10	27	0	0.1>	4	8	0	0.03~0.2	11	59	3	
0.1~0.5	10	49	12	0.1~0.4	19	69	12	0.2~0.4	16	45	9	
0.5~1	9	31	0	0.4~0.7	7	40	0	0.4~0.5	2	12	0	
1~2.5	4	25	0	0.7~1.0	3	15	0	0.5~1.0	4	16	0	
Total	33	132	12	-	33	132	12	-	33	132	12	

$$*\text{Reinforcing index } (R) = \omega_p + \frac{d}{d_p}(\omega_s - \omega'_s) \leq 0.36\beta_1$$

$$\text{where, } \omega_p = \rho_p \frac{f_{pu}}{f'_c}, \omega_s = \rho_s \frac{f_y}{f'_c}, \omega'_s = \rho'_s \frac{f_y}{f'_c}$$

*Notations that are not specifically mentioned can be found in notation part.

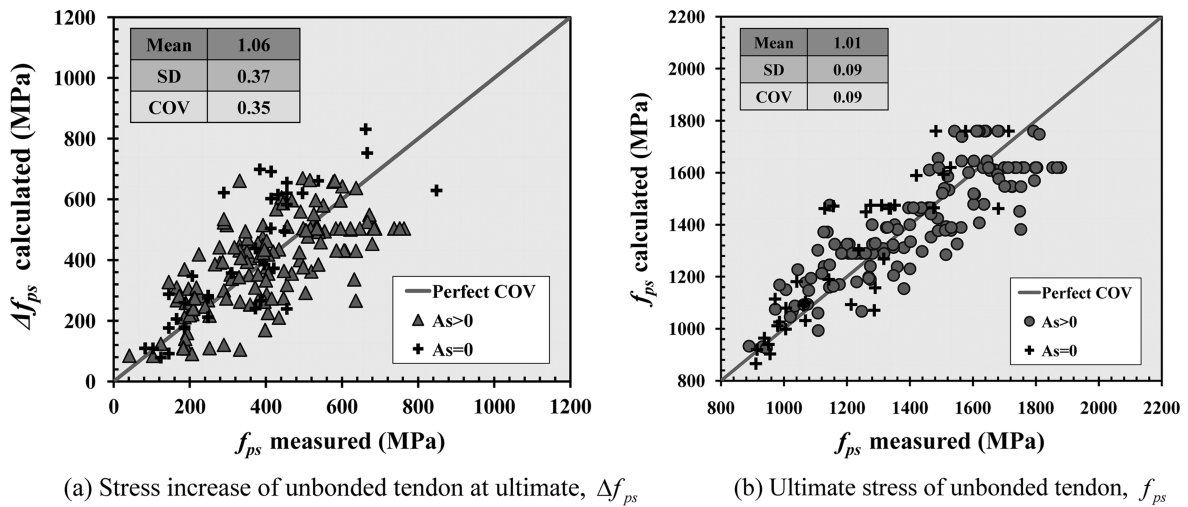


Fig. 12 Performance of the proposed method

Figs. 12(a) and (b) compare the test results and the proposed approach of the increase of tendon stress (Δf_{ps}) and the total tendon stress at ultimate (f_{ps}), respectively. It is shown that both Δf_{ps} and f_{ps} calculated by the proposed approach well match test results. For $\Delta f_{ps, test} / \Delta f_{ps, pred}$ values, the mean average (mean), the standard deviation (SD), and the coefficient of variation (COV) were 1.06, 0.37, and 0.35, respectively; and for $f_{ps, test} / f_{ps, pred}$ values, the mean, SD, and COV were 1.01, 0.09, and 0.09, respectively. It should be noted that, not only for the members with bonded reinforcing bars, but also for those without bonded reinforcing bars, the proposed approach provided Δf_{ps} and f_{ps} very close to the test results. Table 3 shows that the proposed equation is more accurate than the various existing equations that are summarized in Appendix. This implies that the assumption of idealized curvature distribution at ultimate within the maximum moment zone used in the proposed approach works well in most cases.

Fig. 13 compares the test results and the Δf_{ps} and f_{ps} values calculated by the proposed method for 44 UPT members cast with high strength concrete (HSC), over 40 MPa of compressive concrete strength. In addition, Fig. 13 also shows the resulting values from the approach by Ozkul *et al.* (2008), especially proposed for HSC members based on the test results of specimens with concrete compressive strengths of 77~90 MPa. From this approach, the values of mean, SD, and COV of the $\Delta f_{ps, test} / \Delta f_{ps, pred}$ ratios were 0.67, 0.28, and 0.43, respectively, which were 0.91, 0.20, and 0.22, for the proposed method in this study, respectively. This means that the proposed approach yields more accurate results than the equation of Ozkul *et al.* (2008) for the stress increase of tendon at ultimate, which specifically targeted high-strength concrete members.

Figs. 14(a) to (f) show the ratios of the test results to the predicted values ($\Delta f_{ps, test} / \Delta f_{ps, pred}$), from which the performance of the proposed method for the ultimate tendon stress (f_{ps}) with regard to the primary influencing parameters can be examined in more detail. Fig. 14(a) shows the effect of the maximum moment zone length to the member length as well as loading patterns, which reveals that f_{ps} is well predicted by the proposed method without any biased tendency. It means that the assumption on the curvature and the consideration on the loading pattern introduced

Table 3 Performance of various approaches for predicting ultimate tendon stresses

	- Proposed Approach		(a) ACI 318 (2008)		(b) AASHTO-LRFD (2004)	
	$\frac{\Delta f_{ps, test}}{\Delta f_{ps, pred}}$	$\frac{f_{ps, test}}{f_{ps, pred}}$	$\frac{\Delta f_{ps, test}}{\Delta f_{ps, pred}}$	$\frac{f_{ps, test}}{f_{ps, pred}}$	$\frac{\Delta f_{ps, test}}{\Delta f_{ps, pred}}$	$\frac{f_{ps, test}}{f_{ps, pred}}$
Mean	1.06	1.01	0.61	0.85	0.65	0.90
SD	0.37	0.09	0.36	0.08	0.46	0.10
COV	0.35	0.09	0.59	0.10	0.70	0.11
	(c) Bui and Niwa (2006)		(d) Naaman and Alkhairi (1991b)		(e) Lee <i>et al.</i> (1999)	
	$\frac{\Delta f_{ps, test}}{\Delta f_{ps, pred}}$	$\frac{f_{ps, test}}{f_{ps, pred}}$	$\frac{\Delta f_{ps, test}}{\Delta f_{ps, pred}}$	$\frac{f_{ps, test}}{f_{ps, pred}}$	$\frac{\Delta f_{ps, test}}{\Delta f_{ps, pred}}$	$\frac{f_{ps, test}}{f_{ps, pred}}$
Mean	1.03	0.96	0.82	0.91	0.72	0.9
SD	0.87	0.15	0.60	0.09	0.51	0.11
COV	0.84	0.16	0.74	0.10	0.71	0.13
	(f) Harajli and Kanj (1991)		(g) Warwaruk <i>et al.</i> (1962)		(h) Tam and Pannell (1976)	
	$\frac{\Delta f_{ps, test}}{\Delta f_{ps, pred}}$	$\frac{f_{ps, test}}{f_{ps, pred}}$	$\frac{\Delta f_{ps, test}}{\Delta f_{ps, pred}}$	$\frac{f_{ps, test}}{f_{ps, pred}}$	$\frac{\Delta f_{ps, test}}{\Delta f_{ps, pred}}$	$\frac{f_{ps, test}}{f_{ps, pred}}$
Mean	0.71	0.90	0.41	0.83	0.79	0.94
SD	0.38	0.09	0.22	0.08	0.52	0.13
COV	0.54	0.10	0.54	0.10	0.65	0.13
	(i) Robert-Wollmann <i>et al.</i> (2005)		(j) Ozkul <i>et al.</i> (2008)		(k) Du and Tao (1985)	
	$\frac{\Delta f_{ps, test}}{\Delta f_{ps, pred}}$	$\frac{f_{ps, test}}{f_{ps, pred}}$	$\frac{\Delta f_{ps, test}}{\Delta f_{ps, pred}}$	$\frac{f_{ps, test}}{f_{ps, pred}}$	$\frac{\Delta f_{ps, test}}{\Delta f_{ps, pred}}$	$\frac{f_{ps, test}}{f_{ps, pred}}$
Mean	0.68	0.90	1.12	0.97	1.17	1.01
SD	0.48	0.11	0.62	0.09	0.71	0.12
COV	0.70	0.13	0.55	0.10	0.60	0.12

in the proposed approach are reasonable and supportive. Fig. 14(b) shows the effect of span-depth ratio (L/d_p), which reveals that the estimated values well match to the test results in all range of L/d_p , approximately between 8 and 48. This implies that the proposed method works well up to relatively long span members.

Fig. 14(c) shows how well the effect of the amount of the bonded reinforcing bars on f_{ps} , including for the cases without any bonded reinforcing bar, was reflected in the proposed approach. It shows that the effect of bonded reinforcing bars were well considered from the cases without any bonded reinforcing bar and up to about 2.5% of the ratio of the bonded reinforcing bars, which coincides with the previous observation in Fig. 12. Fig. 14(d) shows the effect of the reinforcing index (R) on the performance of the proposed method. Indeed, the values by the proposed method

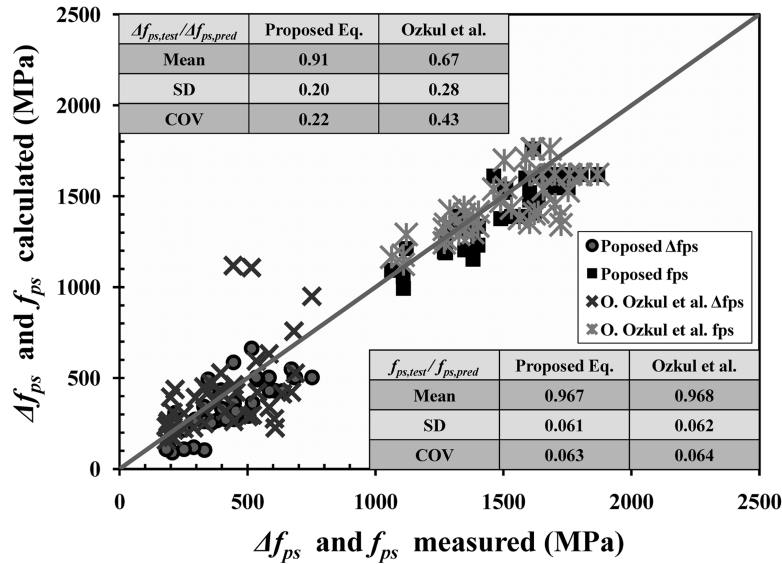


Fig. 13 Estimation of Δf_{ps} and f_{ps} for UPT members cast with high strength concrete

are very close to the test values in all the reinforcing indices. This particularly shows that the proposed equation accurately predicts the strength of specimens whose reinforcing index exceeds the limited value, $0.36\beta_1$ that the 1999 and earlier edition of ACI code (1995) presented to assure ductile tension failure. It is considered that this result is due to the proper consideration of the effect of the amount of tendons and the amount of reinforcing bars in the calculation of the neutral axis and the tendon stress in Eqs. (11) to (15). Therefore, this demonstrates that the proposed equation can also be applied to over-reinforced members, which can often occur during repairs and reinforcing works by external post-tension in construction fields.

Fig. 14(e) examines the effect of the relative stress ratio of the increase of tendon stress due to loading to the initial prestress ($f_{pe, test}$) on the estimation of f_{ps} , in which the larger values of $\Delta f_{ps, test} / \Delta f_{pe, test}$ mean the larger the stress increase due to the applied loading compared to the initial prestress. It also demonstrates that, in the full range of the $\Delta f_{ps, test} / \Delta f_{pe, test}$ values, the estimated values of f_{ps} from the proposed method agree well with the test results.

Fig. 14(f) shows the predicted values of f_{ps} versus the depths of the neutral axis, which was calculated by substituting the f_{ps} from the test results into Eq. (9). The predicted values of f_{ps} in all ranges of neutral axis depths are very close to the test results, which means that the average strain increase of tendons at ultimate ($\Delta \epsilon_{ps}$) from Eq. (15), as proposed in this study, adequately reflects the effect of the neutral axis.

In conclusion, as explained by Figs. 13 and 14, the predicted Δf_{ps} and f_{ps} values proposed in this study adequately consider all the important influencing factors on ultimate tendon stress. Fig. 15 compares the flexural strengths of UPT members predicted by Eq. (18) (M_n Predicted), based on the proposed model for f_{ps} , and the test results (M_n Predicted) reported in the existing literature (Janney *et al.* 1956, Warwaruk *et al.* 1962, Du and Tao 1985, Harajli and Kanj 1991, Campbell and Chouinard 1991, Chakrabarti 1995, Moon *et al.* 2002, Ozkul *et al.* 2005, Ozkul *et al.* 2008). The ratios of the analysis results (M_n Predicted) to the test values (M_n Tested) yield a mean of 1.07, SD

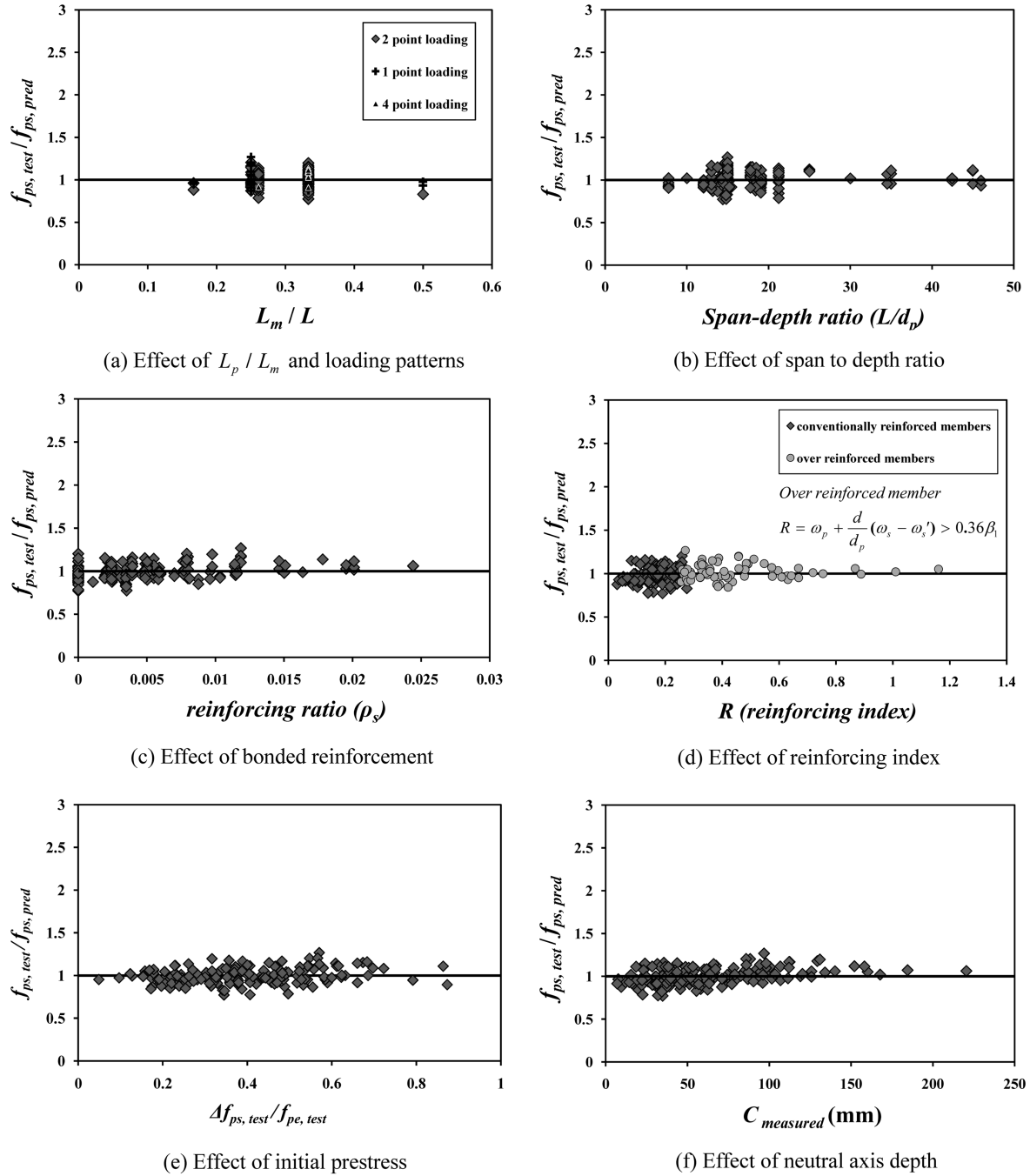


Fig. 14 Performance of the proposed method versus primary influencing parameters

of 0.15, and COV of 0.14, which verifies the good accuracy of the proposed approach for estimation of the flexural strengths of UPT members.

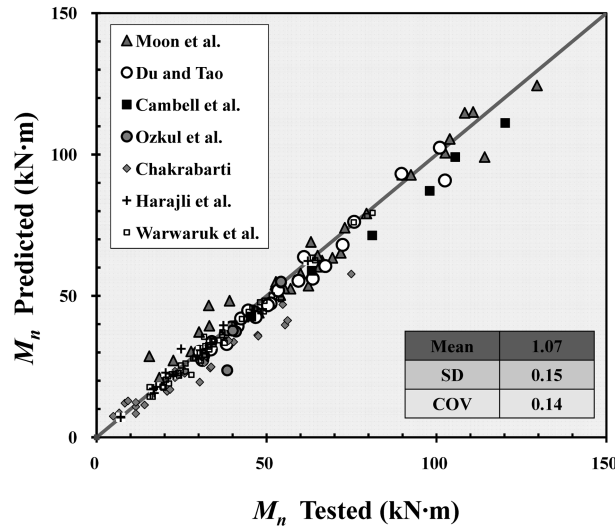


Fig. 15 Estimation of flexural strength of UPT members

6. Conclusions

In this study, the existing approaches for the estimation of ultimate tendon stresses and the flexural strengths of UPT members were examined, and a improved approach was proposed. Also, the accuracy of existing equations and of the proposed equation were evaluated using the database of 177 test results established in this study, from which the following conclusions are made:

1. The proposed method for the estimation of the ultimate stresses of unbonded tendons and the flexural strengths of UPT members showed very good agreement with test results reflecting well the effect of primary influencing parameters, and provided better performance than the existing approaches examined in this study.
2. The assumption of the ultimate curvature in UPT members subjected to two-point loading, in which the ultimate curvature is simplified to be distributed equally within the maximum moment region, and the coefficient of moment shape introduced to consider other loading types are considered to be reasonable from the analysis results. It was also shown that the proposed method can also be applied to the UPT members without bonded reinforcement providing a reasonable estimation of their flexural strengths as well.
3. The approach used in this research of considering the area ratio of moment diagram to account for the effect of various loading patterns allowed the simple and reasonable estimation of the flexural strength of UPT members.
4. The proposed method also provided reasonably good estimation of the flexural strengths of the over-reinforced members, which can often occur when repairing or retrofitting existing structural members.
5. The proposed approach well predicted the flexural strengths of the UPT members cast with not only normal-strength concrete but also high-strength concrete.

Acknowledgements

This work was supported by the Korea Research Foundation Grant funded by the Korean Government (MOEHRD, Basic Research Promotion Fund) (KRF-2008-331-D00637).

References

- ACI Committee 318 (1995), "Building code requirements for structural concrete and commentary (ACI 318M-95)", American Concrete Institute, Farmington Hills, MI.
- ACI Committee 318 (2005), "Building code requirements for structural concrete and commentary (ACI 318M-05)", American Concrete Institute, Farmington Hills, MI.
- ACI Committee 318 (2008), "Building code requirements for structural concrete and commentary (ACI 318M-08)", American Concrete Institute, Farmington Hills, MI.
- Allouche, E.N., Campbell, T.I., Green, M.F. and Soudki, K.A. (1999), "Tendon stress in continuous unbonded prestressed concrete members - Part 1 parametric study", *PCI J.*, **44**(1), 86-93.
- Au, F.T.K. and Du, J.S. (2004), "Prediction of ultimate stress in unbonded tendons", *Mag. Concrete Res.*, **56**(1), 1-11.
- Au, F.T.K., Chan, K.H.E., Kwan, A.K.H. and Du, J.S. (2009), "Flexural ductility of prestressed concrete beams with unbonded tendons", *Comput. Concrete*, **6**(6), 451-472.
- American Association of State Highway and Transportation Officials (2004), "AASHTO LRFD bridge design specifications", Third Edition, AASHTO, Washington, DC.
- Bondy, K.B. (1970), "Realistic requirements for unbonded post-tensioning tendons", *PCI J.*, **15**(1), 50-59.
- Bui, D.K. and Niwa, J. (2006), "Prediction of loading-induced stress in unbonded tendons at ultimate", *Doboku Gakkai Ronbunshu E*, **62**(2), 428-443.
- BSI 8110-85 (1985), "Section 4.3.7.3: structural use of concrete", British Standards Institution, London.
- Campbell, T.I. and Chouinard, K.L. (1991), "Influence of non-prestressed reinforcement on the strength of unbonded partially prestressed concrete member", *ACI Struct. J.*, **88**(5), 546-551.
- CAN3-A23.3-M94 (1994), "Design of concrete structure", Canadian Standard Association, Rexdale, Ontario.
- Chakrabarti, P.R. (1995), "Ultimate stress for unbonded post-tensioning tendons in partially prestressed beam", *ACI Struct. J.*, **92**(6), 689-697.
- Collins, M.P. and Mitchell, D. (1991), *Prestressed Concrete Structures*, Prentice Hall, Englewood Cliffs, NJ.
- DIN 4227 (1980), "Part 6: Prestressed concrete, construction of prestressed concrete member", German Code.
- Du, J.S., Au, F.T.K., Cheung, Y.K. and Kwan, A.K.H. (2008), "Ductility analysis of prestressed concrete beams with unbonded tendons", *Eng. Struct.*, **30**(1), 13-21.
- Du, G. and Tao, X. (1985), "Ultimate stress of unbonded tendons in partially prestressed concrete beams", *PCI J.*, **30**(6), 72-91.
- Harajli, M.H. (1990), "Effect of span-depth ratio on the ultimate steel stress in unbonded prestressed concrete members", *ACI Struct. J.*, **87**(3), 305-312.
- Harajli, M.H. (2006), "On the stress in unbonded tendon at ultimate: critical assessment and proposed change", *ACI Struct. J.*, **103**(6), 803-812.
- Harajli, M.H. and Kanj, M.Y. (1991), "Ultimate flexural strength of concrete members prestressed with unbonded tendons", *ACI Struct. J.*, **88**(6), 663-673.
- Janney, J.R., Hognestad, E. and Mchenry, D. (1956), "Ultimate flexural strength of prestressed and conventionally reinforced concrete beam", *ACI Struct. J.*, **52**(2), 601-620.
- KCI-M-07 (2007), *Design Specifications for Concrete Structures*, Korea Concrete Institute.
- Lee, L.H., Moon, J.H. and Lim, J.H. (1999), "Proposed methodology for computing of unbonded tendon stress at flexural failure", *ACI Struct. J.*, **96**(6), 1040-1048.
- Mojtahedi, S. and Gamble, W.L. (1978), "Ultimate steel stresses in unbonded prestressed concrete", *J. Struct. Div.-ASCE*, **104**(7), 1159-1165.
- Moon, J.H., Lim, J.H. and Lee, C.G. (2002), "Relation of deflection of prestressed concrete members to

- unbonded tendon stress and effect of various parameters”, *J. Korea Concrete Inst.*, **14**(2), 171-179.
- Macgregor, R.J.G., Kregor, M.E. and Breen, J.E. (1989), “Strength and ductility of three span externally post-tensioned segmental box girder bridge model”, Research Report, No. 365-3F, Center for Transportation Research, The University of Texas, Austin, Texas.
- Naaman, A.E. and Alkhairi, F.M. (1991a), “Stress at ultimate in unbonded post tensioning tendons - Part 1: evaluation of the state-of-the-art”, *ACI Struct. J.*, **88**(5), 641-651.
- Naaman, A.E. and Alkhairi, F.M. (1991b), “Stress at ultimate in unbonded post tensioning tendons - Part 2: proposed methodology”, *ACI Struct. J.*, **88**(6), 693-692.
- Ng, C.K. (2003), “Tendon stress and flexural strength of externally prestressed beams”, *ACI Struct. J.*, **100**(5), 644-653.
- NEN 3880 (1984), *Part H: Regulations for Concrete*, Dutch Code, Section 503.1.3.
- Ozkul, O., Nasif, H.H. and Malhas, F. (2005), “Deflection prediction and cracking of beams prestressed with unbonded tendons”, Serviceability of Concrete: A Symposium Honoring Dr. E. G. Nawy, SP-225, American Concrete Institute, Farmington Hills, MI.
- Ozkul, O., Nassif, H., Tanchan, P. and Harajli, M.H. (2008), “Rational approach for predicting stress in beams with unbonded tendons”, *ACI Struct. J.*, **105**(3), 338-347.
- Robert-Wollmann, C.L., Kregor, M.E., Rogosky, D.M. and Breen, J.E. (2005), “Stress in external tendons at ultimate”, *ACI Struct. J.*, **102**(2), 206-213.
- Sivaleepunth, C., Niwa, J., Bui, D.K., Tamura, S. and Hamada, Y. (2006), “Prediction of tendon stress and flexural strength of externally prestressed concrete beams”, *Doboku Gakkai Ronbunshu E*, **62**(1), 260-273.
- Tam, A. and Pannell, F.N. (1976), “The ultimate moment resistance of unbonded partially prestressed reinforced concrete”, *Mag. Concrete Res.* **28**(97), 203-208.
- Tan, K.H. and Tjandra, R.A. (2007), “Strengthening of RC continuous beams by external prestressing”, *J. Struct. Eng.-ASCE*, **133**(2), 195-204.
- Warwaruk, J., Sozen, M.A. and Siess, C.P. (1962), “Investigation of prestressed concrete for highway bridges, part.: strength and behavior in flexure of prestressed beam”, Bulletin No. 464, Engineering Experiment Station, University of Illinois, Urbana, Ill.
- Zhou, W. and Zheng, W.Z. (2010), “Experimental research on plastic design method and moment redistribution in continuous concrete beams prestressed with unbonded tendons”, *Mag. Concrete Res.*, **62**(1), 51-64.

Notations

α	: coefficient of moment shape
β_1	: factor of equivalent rectangular compressive stress block to neutral axis depth
c_m	: neutral axis depth in the maximum moment zone at ultimate
c_y	: neutral axis depth assuming $f_{ps} = f_{py}$
ϵ_{cu}	: ultimate concrete strain
ϵ_{pe}	: effective prestrain in prestressing steel = f_{pe}/E_{ps}
$\Delta\epsilon_{pc}$: strain increase of concrete at the level of tendon after loading
f_c'	: specified compressive strength of concrete
f_{ps}	: ultimate stress of prestressing tendon
f_{pe}	: effective prestress in prestressing steel
f_{pu}	: tensile strength of prestressing steel
f_{py}	: yield stress of prestressing steel
f_s	: stress of tensile reinforcement
f_s'	: stress of compressive reinforcement
f_y	: yield stress of reinforcing steel
ϕ_x	: beam curvature
ϕ_m	: beam curvature at maximum moment zone at ultimate
E_p	: modulus of elasticity of prestressing tendon
E_s	: modulus of elasticity of reinforcing bars
b	: flange width
d	: distance from extrem compression fiber to centroid of tension reinforcement
d'	: distance from extrem compression fiber to centroid of compression reinforcement
d_p	: distance from extrem compression fiber to centroid of prestressing tendon
h	: height of section
L_m	: length of maximum moment region
L_p	: plastic hinge length
A_{ps}	: area of unbonded prestressing tendon
A_s	: area of tensile reinforcing bars
A_s'	: area of compressive reinforcing bars
ϵ_{ps}	: strain of prestressing tendons at ultimate state
ρ_p	: ratio of prestressing tendons = A_{ps}/b_p
ρ_s	: ratio of bonded reinforcing bars = A_s/b_d
ω_s	: tension reinforcement index
ω_s'	: compression reinforcement index
ω_p	: prestressing steel index
R	: reinforcement index
k	: ratio of maximum moment region to beam length
C_c	: compression force of concrete
C_s'	: compression force of reinforcing bar
T_s	: tension force of reinforcing bar
T_{ps}	: tension force of prestressing tendon
M_n	: ultimate moment capacity